

SPECTROPHOTOMETRY OF ASTEROIDS: THE ASSESSMENT OF THE MATERIAL COMPOSITION OF PRIMITIVE ASTEROIDS NEAR PERIHELION

M. P. Shcherbina^{a,b*}, *V. V. Busarev*^{a,b}, *S. I. Barabanov*^b

^a *Sternberg Astronomical Institute of Moscow State University (SAI MSU),
Moscow, Russian Federation*

^b *Institute of Astronomy of the Russian Academy of Sciences,
Moscow, Russian Federation*

Using a qualitative interpretation of the reflectance spectra of asteroids, one can indirectly judge the mineralogy of the surface matter of these bodies. The spectral absorption bands are wide enough for correct interpretation even at low resolution. Thus, it is possible to assess the taxonomic class, as well as the prevailing type of mineralogy (low-temperature or high-temperature). In addition to the classical definition of the spectral type, one can use such a feature of the asteroid as the appearance of a temporary exosphere, which affects the shape of the reflectance spectrum. Recently, the number of events of registration of sublimation activity among primitive asteroids has been increasing. We have obtained and analyzed the reflectance spectra of 12 asteroids of the Main Belt, mainly of primitive type. The aim of the study was to study the influence of the temporal exosphere on the correct determination of the spectral type of the asteroid. If the influence of the exosphere is small, then the correct determination of the asteroid's class was possible. It is concluded that the data on asteroids of an unknown taxonomic class during their perihelion passage may give an incorrect idea of the prevailing type of mineralogy.

Keywords: asteroids –spectrophotometry –reflectance spectrum – sublimation activity

1. INTRODUCTION

Asteroids are ideal objects for spectrophotometric ground-based observations. Mineralogical absorption bands in reflectance spectra of asteroids are wide enough

* E-mail: morskayaa906@yandex.ru

to use a low resolution ($R \sim 100$), which makes it possible to expand the range of the asteroid magnitudes and observe more faint objects. The analysis of the reflectance spectra of asteroids makes it possible to qualitatively assess the prevailing type of mineralogy of their matter, using the classifications of Tholen [1] and Bus-Binzel further referred as SMASS [2]. To check the correctness of such estimates, the features of the reflectance spectra of asteroids are compared with the reflectance spectra of the corresponding groups of meteorites. We use the reflectance spectra of meteorites from open databases such as RELAB (Brown University, USA) [3] and the database of the University of Winnipeg (Canada) [4]. Thus, a qualitative assessment of the mineralogy of each asteroid is based on a comparison of its reflectance spectra with the reflectance spectra of meteorites [5]. But we also admit the possibility of discovering new connections between existing groups of meteorites and classes of asteroids.

The Institute of Astronomy of the Russian Academy of Sciences, together with SAI MSU, participates in the international program "Astronomy in the Elbrus region" on spectral observations of asteroids and comets, including those approaching the Earth, based on the use of the Zeiss-2000 (telescope with a low-resolution spectrograph) at the Terskol branch of INASAN. In December 2020, we obtained and analyzed new reflectance spectra of the main belt asteroids: 13 Egeria, 19 Fortuna, 52 Europe, 102 Miriam, 177 Irma, 200 Dynamene, 201 Penelopa, 203 Pompeia, 250 Bettina, 266 Aline, 379 Huenna and 383 Janina. The purpose of these observations was to study the effect of maximum temperatures on the surface matter of the listed asteroids (which have significant orbital eccentricities), including hydrosilicates and probably ice inclusions.

2. THE QUALITATIVE ASSESSMENT OF THE MINERALOGY OF ASTEROIDS

2.1. 13 Egeria

A brief description of the characteristics of asteroid 13 Egeria is given in Table 1. Here is a summary from other publications. The AKARI (Japanese infrared satellite) mission confirmed the presence of hydrated minerals on Egeria [6]. The observations revealed significant inhomogeneities in the distribution of the chemical and mineralogical composition of the surface matter of the asteroid, which could manifest at different phases of rotation. The inhomogeneity of the surface matter of Egeria could arise during dehydration and heating of the matter in the places where large impact craters were formed [7].

The normalized (at $0.55 \mu\text{m}$ here and further) reflectance spectra are shown in Figure 1. The spectrum has a broad absorption band centered at $0.7 \mu\text{m}$, which

is a sign of the presence of hydrated silicates [5]. However, there are weak bands at $0.52 \mu\text{m}$ (a sign of Fe^{2+}) and $0.62 \mu\text{m}$ (a sign of oxidized metal compounds) [8]. The meteorite analogue, selected according to the similarity of the spectra with the minimum square deviation, is Boriskino (CM2), which corresponds to the low-temperature type of mineralogy of the asteroid's surface matter. However, signs of the presence of components of a high-temperature nature lead to the idea of the inhomogeneity of the substance, which was noted earlier.

2.2. 19 Fortuna

A brief description of the characteristics of asteroid 19 Fortuna is given in Table 1. The reflectance spectra are shown in Figure 2. There is a broad absorption band centered at $0.7 \mu\text{m}$, which is a sign of hydrated silicates [5], as well as weaker absorption bands at 0.44 and $0.62 \mu\text{m}$ [7].

At the same time, there is a sharp increase in reflectivity at wavelengths greater than $0.78 \mu\text{m}$, which is inconsistent with the canonical SMASS spectrum of this asteroid and asteroids of this type. Perhaps the reason is the reflectance and scattering of sunlight from the mobile dusty exosphere of the asteroid, which arose near perihelion.

Meteorite analogue: best match is CM2 class meteorites, i. g. Lonewolf Nunataks (CM2).

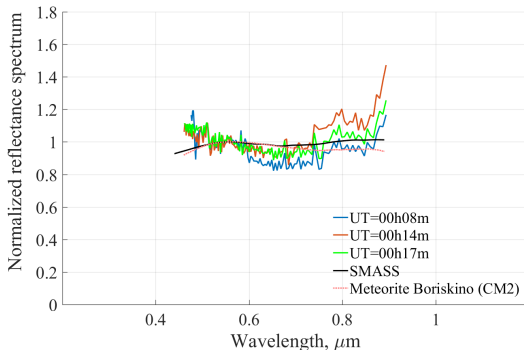


Fig. 1. Reflectance spectra of asteroid 13 Egeria (2020/12/09), reflectance spectrum according to SMASS data and reflectance spectrum of the selected analogue, the meteorite Boriskino (CM2)

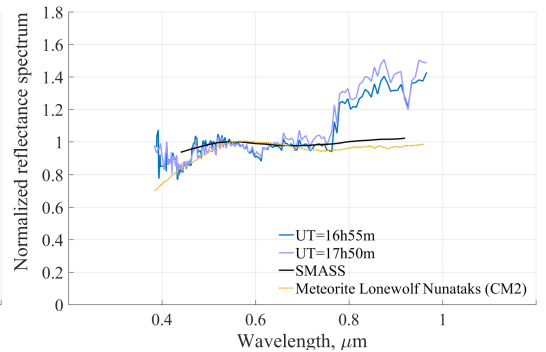


Fig. 2. Reflectance spectra of asteroid 19 Fortuna (2020/12/13), reflectance spectrum according to SMASS data and reflectance spectrum of the selected analogue, the meteorite Lonewolf Nunataks (CM2)

2.3. 52 Europe

A brief description of the characteristics of asteroid 52 Europe is given in Table 1. Here is a summary from other scientific works. The Japanese infrared satellite AKARI has detected the presence of hydrated minerals on Europe [6].

Spectral research also showed the presence of olivine and various pyroxenes in the rocks of the asteroid [9]. The reflectance spectra are shown in Figure 3. The shape of the spectrum is consistent with the C-type. The short-term variability of the spectra can be associated with the presence of a dusty exosphere with the inclusion of ice particles [7]. The selection of meteorite analogues does not provide an unambiguous classification: both representatives of high-temperature mineralogy and low-temperature mineralogy are suitable. This fact indicates a variable composition of the asteroid's surface matter, which is confirmed by other scientific papers cited above.

2.4. 102 Miriam

A brief description of the characteristics of asteroid 102 Miriam is given in Table 1. Originally classified as a D-type asteroid, it was later classified as a C-asteroid, most likely due to the presence of phyllosilicates on the surface [10].

The reflectance spectra are shown in Figure 4. There is a weak band at $0.44 \mu\text{m}$ (a probable sign of the presence of hydrosilicates) [7]. The object rotates extremely slowly, however, in the two spectra we obtained, there are some differences, which can be explained by the result of light scattering by an extremely rarefied dusty exosphere. The selected meteorite analogue Lewis Cliff (CM2) is in a good agreement with the spectrum of the asteroid, confirming the low-temperature nature of the surface matter.

2.5. 177 Irma

A brief description of the characteristics of asteroid 177 Irma is given in Table 1.

The reflectance spectra are shown in Figure 5. There is a broad absorption band at $0.7 \mu\text{m}$ (which is a sign of the presence of hydrated silicates) [5], as well as a weak band at $0.44 \mu\text{m}$. In addition, a short-term change and growth with wavelength of all reflectance spectra may indicate the presence of a temporary dusty exosphere. The reflectance spectrum of the asteroid is in good agreement at shorter wavelengths with the reflectance spectra of many samples of CM2 meteorites, for example, Elephant (CM2), but there is some agreement with the reflectance spectra of other types of meteorites, implying a higher temperature mineralogy.

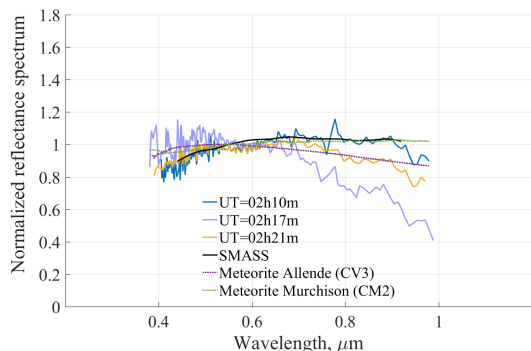


Fig. 3. Reflectance spectra of asteroid 52 Europe (2020/12/08), reflectance spectrum according to SMASS data and reflectance spectra of the selected analogues, the meteorites Allende (CV3) and Murchison (CM2)

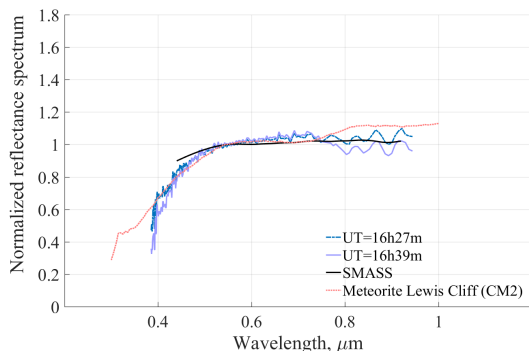


Fig. 4. Reflectance spectra of asteroid 102 Miriam (2020/12/08), reflectance spectrum according to SMASS data and reflectance spectrum of the selected analogue, the meteorite Lewis Cliff (CM2)

2.6. 200 Dynamene

A brief description of the characteristics of asteroid 200 Dynamene is given in Table 1. Spectra of the asteroid show signs of hydrated compounds [11].

The reflectance spectra are shown in Figure 6. The shape of the reflectance spectra of Dynamene does not coincide with the SMASS spectrum. Apparently, such a change in the reflectance spectrum is associated with the scattering of light in the exosphere of silicate particles [7]. It was not possible to select a meteorite analogue, as well as to identify some absorption bands.

2.7. 201 Penelopa

A brief description of the characteristics of asteroid 201 Penelopa is given in Table 1. Even though the asteroid belongs to the class M, it contains a significant amount of silicate components [12]. The presumed presence of phyllosilicates on the surface is due to the water change of high-temperature silicates [12].

The reflectance spectra are shown in Figure 7. There is a weak absorption band at 0.7 μm , which indicates the presence of hydrated silicates [5]. The selection of a meteorite analogue shows correspondence with different types of meteorites, which is an additional sign of a mixed composition of the surface matter.

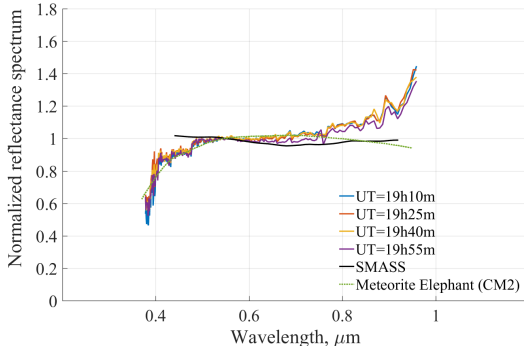


Fig. 5. Reflectance spectra of asteroid 177 Irma (2020/12/13), reflectance spectrum according to SMASS data and reflectance spectrum of the selected analogue, the meteorite Elephant (CM2)

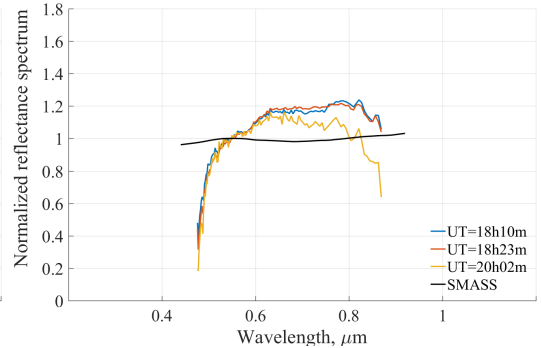


Fig. 6. Reflectance spectra of asteroid 200 Dynamene (2020/12/11) and reflectance spectrum according to SMASS data. It was not possible to select a meteorite analogue

2.8. 203 Pompeia

A brief description of the characteristics of asteroid 203 Pompeia is given in Table 1. Previously, other researchers did not assess the belonging of this asteroid to any taxonomic class. However, it turned out that the visible spectrum of the asteroid has a pronounced red color, which is more characteristic of objects in the Kuiper belt, and not for asteroids in the main belt. This feature of the spectrum is explained by the outer organic-rich layer on its surface and the fact that it could have formed in the outer part of the solar system outside the asteroid belt [13].

The reflectance spectra are shown in Figure 8. The spectrum view corresponds to C-type. There is possibly a very weak absorption band at $0.44 \mu\text{m}$, connected possibly with presence of hydrated silicates [7]. Growth in the long-wavelength part may be due to the presence of a combined exosphere (ice-silicates-organic). The selected meteorite counterpart meets the expectations for a low temperature class C (Elephant (CM2)).

2.9. 250 Bettina

A brief description of the characteristics of asteroid 250 Bettina is given in Table 1. Classes of meteorites consistent with the asteroid class are iron meteorites, possibly with silicate inclusions; enstatite chondrite.

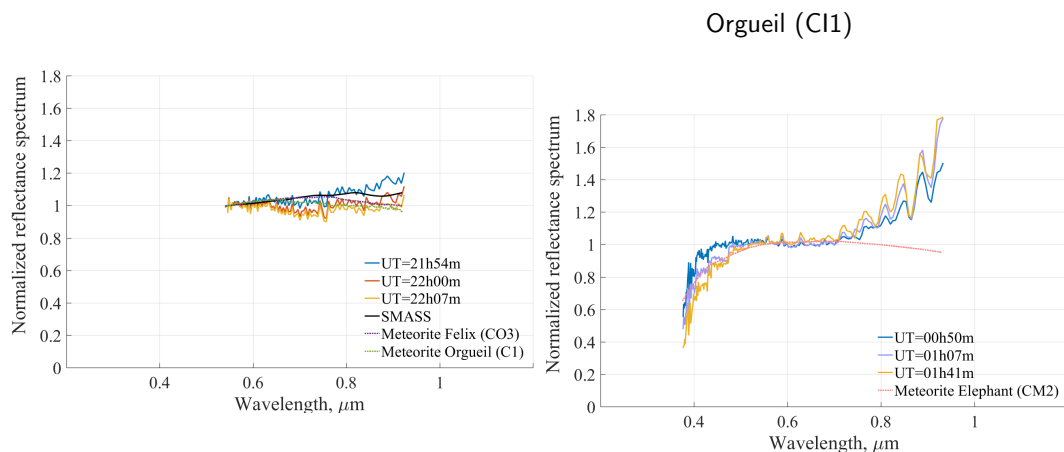


Fig. 7. Reflectance spectra of asteroid 201 Penelopa (2020/12/08), reflectance spectrum according to SMASS data and reflectance spectra of the selected analogues, the meteorites Felix (CO3) and

Fig. 8. Reflectance spectra of asteroid 203 Pompeia (2020/12/14) and reflectance spectrum of the selected analogue, the meteorite Elephant (CM2)

The reflectance spectra are shown in Figure 9. The shape of the reflectance spectrum corresponds to the SMASS spectrum, and the selected meteorite analogue is well suited to this taxonomic class of the asteroid (Jiddat al Harasis (Euclite)).

2.10. 266 Aline

A brief description of the characteristics of asteroid 266 Aline is given in Table 1.

The reflectance spectra are shown in Figure 10. The shape of the spectrum corresponds to the reflectance spectrum of class C. There is an increase in the range of 0.85-0.9 μm , which may be a sign of a dusty exosphere. The selected meteorite analogues that showed the best similarity to the asteroid's reflectance spectrum are Elephant (CM2) and Orgueil (CI1), which is an additional indication of the correctness of the asteroid's class estimate.

2.11. 379 Huenna

A brief description of the characteristics of asteroid 379 Huenna is given in Table 1. This asteroid has a satellite orbiting its parent body at a significant distance, about 3400 kilometres. In 2011, studies of the spectra of Guenna and its

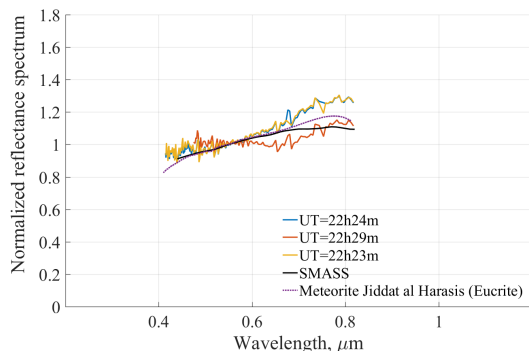


Fig. 9. Reflectance spectra of asteroid 250 Bettina (2020/12/10), reflectance spectrum according to SMASS data and reflectance spectrum of the selected analogue, the meteorite Jiddat al Harasis (eucrite)

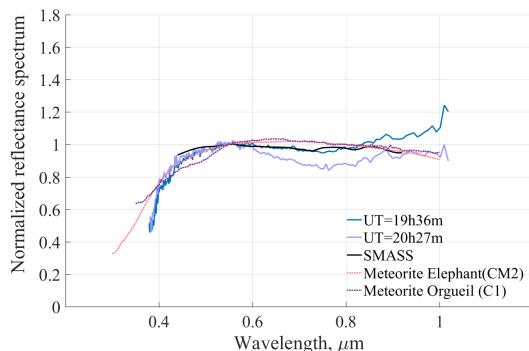


Fig. 10. Reflectance spectra of asteroid 266 Aline (2020/12/10), reflectance spectrum according to SMASS data and reflectance spectra of the selected analogues, the meteorites Elephant (CM2) and Orgueil (C1)

satellite, carried out by an international group of scientists from several countries, were published. According to the research results, it was suggested that S / 2003 (379) 1 is either a fragment of Guenna, or a former member of the Themis family, which became its companion because of gravitational capture [14].

The reflectance spectra are shown in Figure 11. The reflectance spectrum has an indication of the presence of hydrosilicates in the composition of the surface substance, namely, it has an absorption band near $0.7 \mu\text{m}$ [5]. The change in the reflectance spectrum can be caused by the appearance of a predominantly icy exosphere [15]. It was not possible to select a meteorite analogue.

2.12. 383 Janina

A brief description of the characteristics of asteroid 383 Janina is given in Table 1.

The reflectance spectra are shown in Figure 12. The reflectance spectrum has probably an absorption band at $0.44 \mu\text{m}$. Some coincidence of the short-wavelength part of the spectra among meteorite analogues was shown by meteorites of the C1I and CM2 classes, which may be confirmation of the low-temperature mineralogy of the asteroid.

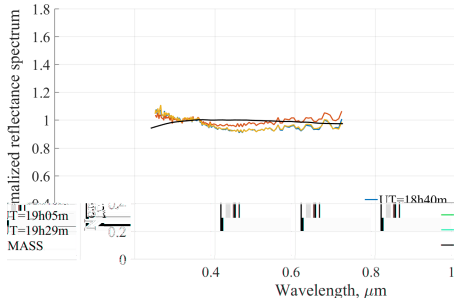


Fig. 11. Reflectance spectra of asteroid 379 Huenna (2020/12/08) and reflectance spectrum according to SMASS data. It was not possible to select a meteorite analogue

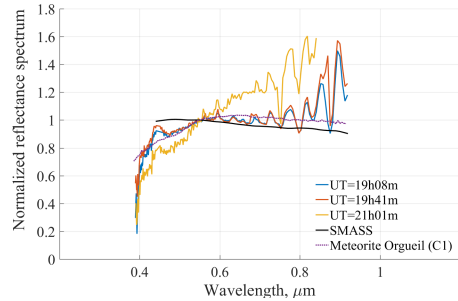


Fig. 12. Reflectance spectra of asteroid 383 Janina (2020/12/07), reflectance spectrum according to SMASS data and reflectance spectrum of the selected analogue, the meteorite Orgueil (C1)

3. CONCLUSION

Almost all considered asteroids (except for the M-type asteroids 201 Penelope and 250 Bettina) may have low-temperature mineralogy (typical minerals are hydrosilicates with probable inclusions of water ice). It could be based on the previously defined taxonomic class C. We deliberately chose the time of observations so that all these bodies were near the perihelion, where their sublimation activity and the formation of a dusty exosphere were possible [15], [16], [17]. Therefore, we probably obtained the reflectance spectra of these asteroids, partially distorted by the influence of a rarefied dusty exosphere, consisting of submicron conglomerates of particles of ice, silicate and tholins’s composition. The effect of such dusty exosphere on the reflectance spectra of asteroids is in good agreement with the modelling of light scattering by the above components [17]. If such distortions were insignificant, then it is possible to estimate taxonomic types and mineralogy of the considered asteroids mainly by the short-wavelength part of these spectra. The estimates obtained are in good agreement with the known data on these objects, as well as with geometric albedo and reflectance spectra of meteorites of proper groups.

It was not always possible to find a suitable meteorite analogue for asteroid spectra. This may be due to both the mixed composition of the asteroid’s surface matter and the incompleteness of the terrestrial collections of meteorite’s matter.

For 203 Pompeia, the spectral type was assessed for the first time.

Table 1. A brief description of the characteristics of asteroids [18]

Asteroid	Day of observation	Confirmed class	Diameter,m	Albedo	Rotation period,hrs
13 Egeria	2020 12 09	G (Ch)	207.64	2	7.05
19 Fortuna	2020 12 13	G (Ch)	200	0.037	7.44
52 Europe	2020 12 08	C	302.5	0.0578	5.63
102 Miriam	2020 12 08	C	83	0.0507	23.61
177 Irma	2020 12 13	Ch	73.22	0.0527	13.86
200 Dy-namene	2020 12 11	Ch	128.36	0.0533	37.39
201 Penelopa	2020 12 08	X (M)	68.39	0.1604	3.74
203 Pom-peia	2020 12 14	?	116.25	0.041	24.05
250 Bettina	2020 12 10	Xk (M)	79.75	0.2581	5.05
266 Aline	2020 12 10	Ch (C)	109.09	0.0448	13.02
379 Huenna	2020 12 08	C	92.33	0.0587	14.14
383 Janina	2020 12 07	B	45.52	0.0926	6.40

The research was supported by the Russian Science Foundation (project RSF No. 22-12-00115).

REFERENCES

1. Tholen D. J., Asteroids II, 1989, 1139-1150
2. Bus S. J., Binzel R. P., Icarus, 2002, **158**, 146-177
3. NASA REFLECTANCE EXPERIMENT LABORATORY, URL: <http://apps.geology.brown.edu/index.php>, last accessed 13 November 2021

4. CENTER FOR TERRESTRIAL AND PLANETARY EXPLORATION, URL: <https://www.uwinnipeg.ca/c-tape/>, last accessed 13 November 2021
5. Gaffey M. J., AIP Conference Proceedings, 2011, **1386**, 129-169
6. Usui F. et al., Publications of the Astronomical Society of Japan, 2019, **71**, 1
7. Busarev V. V. et al., Icarus, 2015, **262**, 44-57
8. Fernandes C., The Open University, 2012, 204
9. Dotto E. et al., Astronomy and Astrophysics, 2000, **358**, 1133-1141
10. Fitzsimmons A. et al., Astronomy and Astrophysics, 1994, **282**, 634-642
11. Fornasier S. et al., Astronomy and Astrophysics Supplement Series, 1999, **135**, 65-73
12. Busarev V. V., Icarus, 1998, **131**, 32-40
13. Hasegawa S. et al., The Astrophysical Journal Letters, 2021, **916**, L6
14. DeMeo F. E. et al., Icarus, 2011, **212**, 677-681
15. Busarev V. V., Barabanov S. I., Puzin V. B., Solar System Research, 2016, **50**, 281-293
16. Busarev V. V. et al., Solar System Research, 2019, **53**, 261-277
17. Busarev V. V. et al., Icarus, 2021, **369**, 11463468-70
18. JPL Small-Body Database, URL: <http://ssd.jpl.nasa.gov/ssdb.cgi>, last accessed 13 November 2021